Металлофиз. новейшие технол. / Metallofiz. Noveishie Tekhnol.
2014, т. 36, № 12, сс. 1609–1619
Оттиски доступны непосредственно от издателя
Фотокопирование разрешено только
в соответствии с лицензией

МЕТАЛЛИЧЕСКИЕ ПОВЕРХНОСТИ И ПЛЁНКИ

PACS numbers: 61.05.cp, 66.30.Pa, 68.35.Fx, 68.37.Lp, 68.37.Ps, 81.10.Jt, 82.80.Ms

Low-Temperature Interdiffusion and Ordered Phase Formation in Au/Cu Nanocrystalline Thin Films at the Different Atmospheres

A. A. Tynkova, S. I. Sidorenko, I. E. Kotenko, V. L. Svetchnikov*, and S. M. Voloshko

National Technical University of Ukraine 'KPI',
37 Peremogy Avenue,
03056 Kyiv, Ukraine
**G. V. Kurdyumov Institute for Metal Physics, N.A.S. of Ukraine,*
36 Academician Vernadsky Blvd.,
UA-03680 Kyiv-142, Ukraine

Interdiffusion processes in the polycrystalline Au (30 nm)/Cu (40 nm) thin films during annealing at 100–200°C for 15 and 30 min in a vacuum with different residual-atmosphere pressures of 10^{-2} and 10^{-6} Pa and in an environment of hydrogen at a pressure of $5 \cdot 10^2$ Pa are investigated. Secondary neutral mass spectrometry complemented with transmission electron microscopy, X-ray diffraction, and atomic force microscopy is used. The intermixing of two layers is observed at the temperatures, at which the bulk diffusion can be safely ruled out. Within the Au layer, the detected Cu profiles and their time evolution are typical *C*-kinetic regime grain boundary profiles. Due to the much higher grain boundary diffusivity, the saturation of Au grain boundaries at the Au-rich side is hit in a very short time. The high Cu concentration level in the Au-side could be interpreted by supposing existing boundaries, which are moving and leaving behind themselves the areas with high Cu concentration close to the stoichiometric compositions. Phase formation takes place in and around grain boundaries due to diffusing component transport along moving grain boundaries.

Досліджено процеси взаємної дифузії в тонких полікристалічних плівках Au (30 нм)/Cu (40 нм) під час відпалу за температур у 100–200°C впродовж 15 і 30 хв. у вакуумі при різних тисках залишкової атмосфери у 10^{-2} і 10^{-6} Па та в середовищі водню при значенні тиску у $5 \cdot 10^2$ Па. Застосовано методу мас-спектрометрії вторинних нейтральних частинок, доповнену трансмісійною електронною мікроскопією, Рентґеновою дифракцією й атомно-силовою мікроскопією. Перемішування двох шарів спостерігалося при температурах, за яких повністю виключається дифузія за об'ємним механізмом. Одержані для шару Au профілі Cu та їх еволюція з часом були типовими профілями *C*-кінетичного режиму зерномежової

дифузії. Внаслідок значно вищої зерномежової дифузійної рухливости в збагаченому шарі Au насичення меж зерен золота досягається за дуже короткий час. Високий рівень концентрації Cu в шарі Au можна пояснити, припускаючи наявність рухливих меж, які залишають поза собою області з високою концентрацією Cu, близькою до стехіометричного складу. Фазоутворення відбувається всередині та навколо меж зерен шляхом переміщення компонента, що дифундує, вздовж рухомих меж зерен.

Исследованы процессы взаимной диффузии в тонких поликристаллических плёнках Au (30 нм)/Cu (40 нм) во время отжига при температурах 100–200°C в течение 15 и 30 мин в вакууме при различных давлениях остаточной атмосферы 10^{-2} и 10^{-6} Па и в среде водорода при давлении $5 \cdot 10^2$ Па. Использован метод масс-спектрометрии вторичных нейтральных частиц, дополненный трансмиссионной электронной микроскопией, рентгеновской дифракцией и атомно-силовой микроскопией. Перемешивание двух слоёв наблюдалось при температурах, при которых объёмная диффузия полностью исключается. Измеряемые для слоя Au профили Cu и их развитие с течением времени были типичными профилями зернограничной диффузии с кинетикой *C*-типа. Из-за гораздо более высокой зернограничной диффузионной подвижности в обогащённом слое Au насыщение границ зёрен золота достигается за очень короткое время. Высокий уровень концентрации Cu в слое Au можно объяснить, предполагая наличие подвижных границ, которые оставляют позади себя области с высокой концентрацией Cu, близкой к стехиометрическому составу. Фазообразование происходит внутри и вокруг границ зёрен посредством перемещения диффундирующего компонента вдоль движущихся границ зёрен.

Key words: grain boundary diffusion, ordered phase, AuCu, thin film, Secondary Neutral Mass Spectrometry.

(Received July 17, 2014)

1. INTRODUCTION

Bilayer and multilayer thin films of platinum group metals and noble metals have become an area of much current research because of their fundamental interest and also their importance in modern device fabrication for technological applications, such as microelectronic devices, sensors, coatings, magnetic recording, *etc*. [1–3]. The performance and stability of such devices can be improved or damaged by interdiffusion and accompanying reactions between adjacent metal layers [4–6]. Therefore, a fundamental understanding of the diffusion processes in the thin-film systems is of major importance.

In general terms, interdiffusion in the thin-film systems takes place through lattice defects such as vacancies, dislocations, and grain boundaries. Depending on the pathways followed by the diffusing species, *e.g.*, bulk or grain boundaries, diffusion can be classified according to three kinetic regimes: *A*, *B*, or *C* [7], as schematically depicted in

Fig. 1. The *A*-regime refers to abundant atomic migration from the boundaries into the grains. The *B*-kinetics describes a limited diffusion from the grain boundaries into the grains; in this case, a combination of bulk and grain boundary diffusion occurs. Finally, the *C*-kinetics refers to purely grain boundaries diffusion and the bulk contribution is negligible [8].

It is known that at low temperatures, where the bulk diffusion processes are practically frozen, even a complete intermixing of components in the thin film bilayer structures can happen by grain-boundary (GB) diffusion and GB migration through the film bulk [9, 10]. The interdiffusion is often accompanied with the formation of the compound phases [11–13]. As an example, in the Cu/Pd system, it was observed by transmission electron microscopy (TEM) that the original interface between the Cu and Pd layers remained clearly visible at 473 K, but the selected area diffraction patterns in TEM indicated the presence of the PdCu phase in GBs [14].

In Ref. [15], the early stages of the interreaction and interdiffusion in Cu (150 nm)/Au (150 nm) system after annealing at 330°C were investigated by hollow cone dark field imaging. It was observed that interdiffusion is not homogeneous along the interface and there is no indication that the Cu_3Au phase is formed at the very beginning of interreaction, which may be related to the stress caused by the lattice mismatch.

The Au/Cu thin films were investigated in the temperature range of 100–250°C in vacuum and hydrogen atmosphere [16]. X-ray diffraction revealed the predominance of the Cu-rich phase Cu_3Au in the hydrogen ambient, while phases richer in Au are relatively more preva-

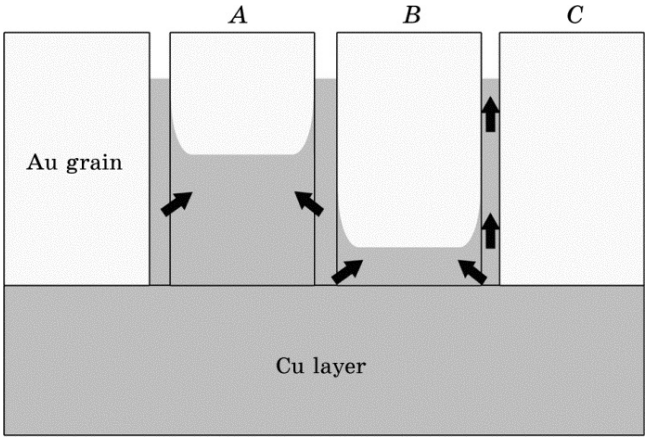

Fig. 1. Schematic representation of the three kinetic regimes (*A*, *B*, and *C*) of diffusion in the polycrystalline systems for the case of Cu diffusing into Au thin films.

lent in the air ambient. The difference is explained by a model, in which both bulk and grain boundary diffusion mechanisms are operative and a certain proportion of the Cu atoms diffusing along the grain boundaries is trapped by oxidation in the air ambient before they can diffuse into the grains.

In the present work, the influence of residual atmospheres on the interdiffusion and phase formation processes in thin bilayer diffusion couples of Au and Cu has been investigated employing secondary neutral mass spectrometry (SNMS) as one of the most powerful methods used for determination of the grain boundary diffusion parameters in thin films in combination with X-ray diffraction (XRD), TEM, and atomic force microscopy (AFM). It has been found that at 200°C, where the bulk diffusion transport is completely frozen, new ordered phase Cu_3Au formed by supposing moving GBs and, for example, diffusion induced grain boundaries migration (DIGM) process.

2. EXPERIMENTAL DETAILS

Polycrystalline Au (30 nm)/Cu (40 nm) samples were resistively deposited without breaking vacuum $5 \cdot 10^{-2}$ Pa onto glass substrate kept under room temperature. Samples were annealed at 100°C and 200°C for 15 and 30 min in vacuum 10^{-2} Pa, 10^{-6} Pa and in hydrogen atmosphere at a pressure of $5 \cdot 10^{2}$ Pa.

The concentration profiles are measured by SNMS (SPECS INA-X) using noble gas plasma and ion current with an extremely high lateral homogeneity. The low bombarding energies (about 100 eV) and the homogeneous plasma profile result in an outstanding depth resolution (< 2 nm). Details of the SNMS device and the profile evaluation can be found elsewhere [17, 18]. X-ray studies are performed with Siemens D5000 under the grazing angle 3° in CuK_α radiation using parallel alignment with X-ray mirror.

A study of the microstructures and cross-sectioned samples is performed by TEM (SELMI PEM-125K). High-energy electron diffraction is performed at 75 kV with EMR-100 electron diffraction unite.

A surface topography of the samples is investigated using NanosurfMobileS AFM microscope.

3. RESULTS AND DISCUSSION

Au/Cu concentration profiles of the as-deposited and annealed samples are shown in Fig. 2. We observe well-developed Cu diffusion to Au layer at as-deposited state that takes place during the sample preparation. Such factors as surface roughness and instrumental effects of the sputter depth profiling play the minor role in this case [18]. It can be

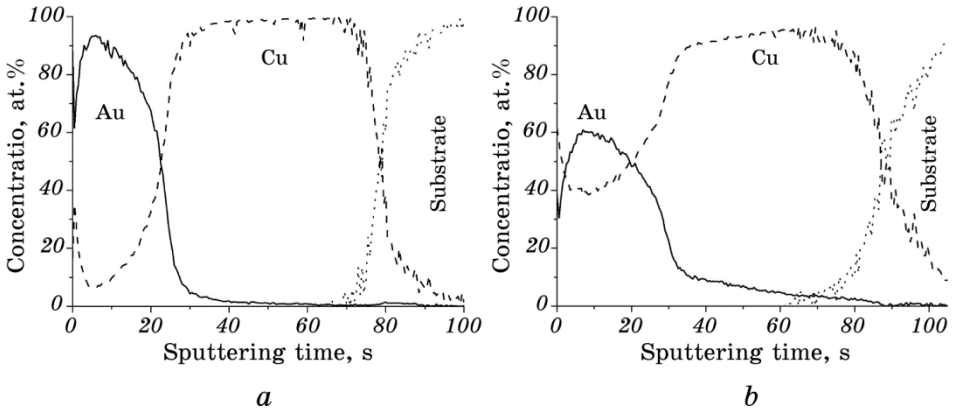

Fig. 2. Concentration profiles of Au (30 nm)/Cu (40 nm) system as deposited (*a*); after annealing at 100°C for 30 min in vacuum under the pressure $P = 10^{-2}$ Pa (*b*).

clearly seen that during heat treatments the Au penetration into the Cu layer is less intensive. This can be explained by the grain boundary diffusivity of the components: $D_{Au \to Cu} = 1.2 \cdot 10^{-17}$ m^2/s, $D_{Cu \to Au} = 1.2 \times \times 10^{-16}$ m^2/s [19, 20].

The most significant intermixing occurs on the Au-side during annealing in vacuum under the pressure $P = 10^{-2}$ Pa, with the concentration of Cu up to 40 at.%, while on the Cu-side the concentration of Au atoms reaches only 10 at.% (Fig. 2, *b*). The diffusion processes of the elements after heat treatments in high vacuum and in hydrogen atmosphere are comparable with those that are observed in as-deposited sample, thus they are not shown. Annealing in high vacuum leads to the concentration up to 9 at.% and 1 at.% for Cu in Au layer and Au for Cu layer, respectively. After annealing in hydrogen atmosphere, the concentration reaches only 11 at.% for Cu and 1 at.% for Au atoms.

The overall composition of the diffusing elements on both sides is rather high and cannot be explained by a simple filling up of grain boundaries (assuming that the GBs are completely filled by the diffusing atoms). It could be attributed to the fact that the observed values are much higher than the average value estimated from the grain size (see the TEM picture in Fig. 3). The grain size of Au is about 10 nm, and, for the case of Cu, it is of 15 nm. The complete filling of GBs would lead to a maximum average composition of about 5 at.% and 3 at.% for Au and Cu, respectively (assuming δ/d for the GB fraction, where $\delta = 0.5$ nm is the grain-boundary thickness).

It is worth to emphasize that we did not observe a reaction layer at the original interface in concentration profiles. It indicates that instead of nucleation of the product layer at the original interface, the

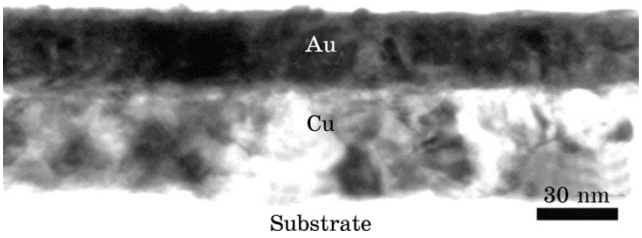

Fig. 3. Cross-section TEM picture of Au (30 nm)/Cu (40 nm) system at as-deposited state.

new phases are formed in the whole volume of the films. The compound phases have been formed without input of the bulk diffusion. According to the tracer data of Maier [21], Cu bulk self-diffusion coefficients at temperatures 150°C and 250°C are $5 \cdot 10^{-30}$ m^2/s and $2.2 \cdot 10^{-25}$ m^2/s, respectively. Taking into account the annealing time in our case (t = = 900 s), the bulk penetration depth ($(DT)^{1/2}$) at 150°C is $4.5 \cdot 10^{-18}$ m. It means that the condition of C-kinetic regime is strictly fulfilled, $(DT)^{1/2} << \delta$, *i.e.* the transport in Cu below 150°C is restricted to the grain boundaries only.

The AFM pictures of Au (30 nm)/Cu (40 nm) samples before and after annealing in vacuum under the pressure $P = 10^{-2}$ Pa are shown in Fig. 4. As it follows from AFM measurements, a roughness of the surface is raising from 11.97 nm as compare with the initial state (7.55 nm). It corresponds to SNMS data that confirms the appearance of some Cu at the topmost surface. It indicates that along fast boundaries or triple junctions Cu atoms are also able to reach the Au surface. The coexistence of the fast and slow diffusion boundaries explains not only the appearance of Cu atoms at the topmost surface, but the formation

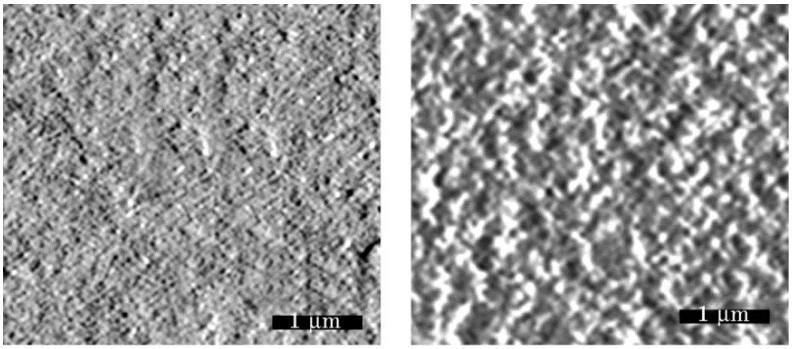

Fig. 4. AFM images for the Au/Cu system surface at as-deposited state (*a*) and after annealing at 100°C for 30 min in a vacuum at the pressure of 10^{-2} Pa (*b*).

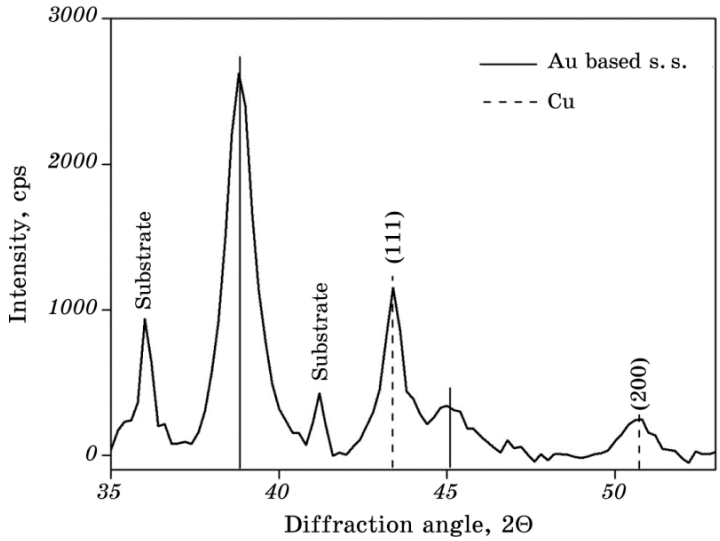

Fig. 5. XRD Θ–2Θ patterns of Au/Cu as-deposited sample.

of a concentration minimum in the Au layer as well: Cu atoms that are transported along fast GBs form a secondary diffusion source at the surface. Since the fast GBs are saturated, the backward transport from the surface may take place along the 'empty' slow boundaries only. The appearance of the minimum in observed concentration depth profile is a result of the averaging process, and it does not mean an 'uphill diffusion' [22].

The XRD pattern of as-deposited sample is shown in Fig. 5. The reflections at 38.6° and 45° indicate the presence of Au-based solid solution formed during the sample preparation procedure. After annealing under different conditions, the peaks do not change their positions as compare with as-deposited state, thus these results are not present.

The Cu concentrations in Au-based solid solutions are calculated from the lattice constants derived from the *X*-ray data collected after annealing. These are shown in Table 1. The amount of the dissolved Cu after annealing under the vacuum of 10^{-2} Pa is 14 at.%, which is much higher than after annealing in either the vacuum at 10^{-6} Pa (12 at.%) or in the hydrogen atmosphere (10 at.%). The grain size L of Au-based solid solution is estimated from the full width at half maximum (FWHM) of the (111) peak using Debye–Scherrer formula [23]:

$$L = \frac{0.9\lambda}{\beta \cos\theta}, \tag{1}$$

where β is the FWHM, λ is the wavelength of CuK_α radiation and θ is the angle of diffraction.

TABLE 1. Values of Cu concentration in Au-based solid solution and grain size of formed Au-based solid solution before and after annealing at 100°C for 30 min in different atmospheres as calculated from XRD.

Annealing conditions	Amount of dissolved Cu, at.%	$L_{\text{Au s.s.}}$ (grain size), nm
As-deposited state	12	10
$P = 10^{-2}$ Pa	14	18
$P = 10^{-6}$ Pa	12	10.1
Hydrogen	11	9.8

Figure 6 shows bright field (top view) TEM images and selected area electron diffraction patterns of as received and heat-treated Au (30 nm) Cu (40 nm) bilayers, respectively. It is seen that there is detectable change in the grain size after the heat treatment. The diffraction pattern of as deposited sample shows clear reflections from Au and Cu (Fig. 6, *b*), and after annealing additional diffraction spots are found that correspond to the ordered Cu_3Au phase (Fig. 6, *d*).

XRD investigation of the same sample proves the presence of the ordered Cu_3Au phase (Fig. 7). Thus, the amount of this phase is small; the peak corresponding to Cu_3Au is weak. Meanwhile, the amount of dissolved Cu reaches 88 at.% and reflections that belong to pure Cu disappear.

Presented results indicate a special way of nucleation and growth of homogeneous reaction products in AuCu system. The formation of reaction layers took place along GBs, and after annealing at higher temperature even the superlattice reflections of the ordered Cu_3Au phase cab be detected only in the case of the treatment in vacuum 10^{-2} Pa. DIGM and diffusion-induced re-crystallization (DIR) are the examples of such kind of GB motions. It is rather difficult to distinguish DIR and DIGM experimentally (see, for example [24]). It is more and more widely accepted that in both processes the driving forces are related to stress accumulation and relaxation ahead/around the moving boundary [9, 25]. In case of low temperature processes (when there is no bulk diffusion), it is most likely to suppose that the migrating GB driving force is originated by the diffusion induced GB stresses created by the differences of the GB atomic fluxes of the two components [26]. We did not observe any phase formation after annealing neither in hydrogen atmosphere, nor under vacuum 10^{-6} Pa. In accordance with the results of [14, 27–29], the observations cannot be understood as a planar layer reaction, thus no continuous reaction layer is formed at the original interface.

The calculated values of the grain size (see Table 1) indicate that some recrystallization took place during annealing only in vacuum 10^{-2} Pa. As we observe from TEM measurements, heat treatment at higher

temperature also leads to the further grain growth (Fig. 6). Taking into account that the bulk diffusion is negligible at these temperatures, we can conclude that all these phenomena should be the result of the grain boundary transport.

Thus, the GB diffusion initiates the nucleation of the reaction product and sweeps the GBs perpendicular to the original surface and, as a result, an alloyed zone remains behind the moving GBs. The obtained

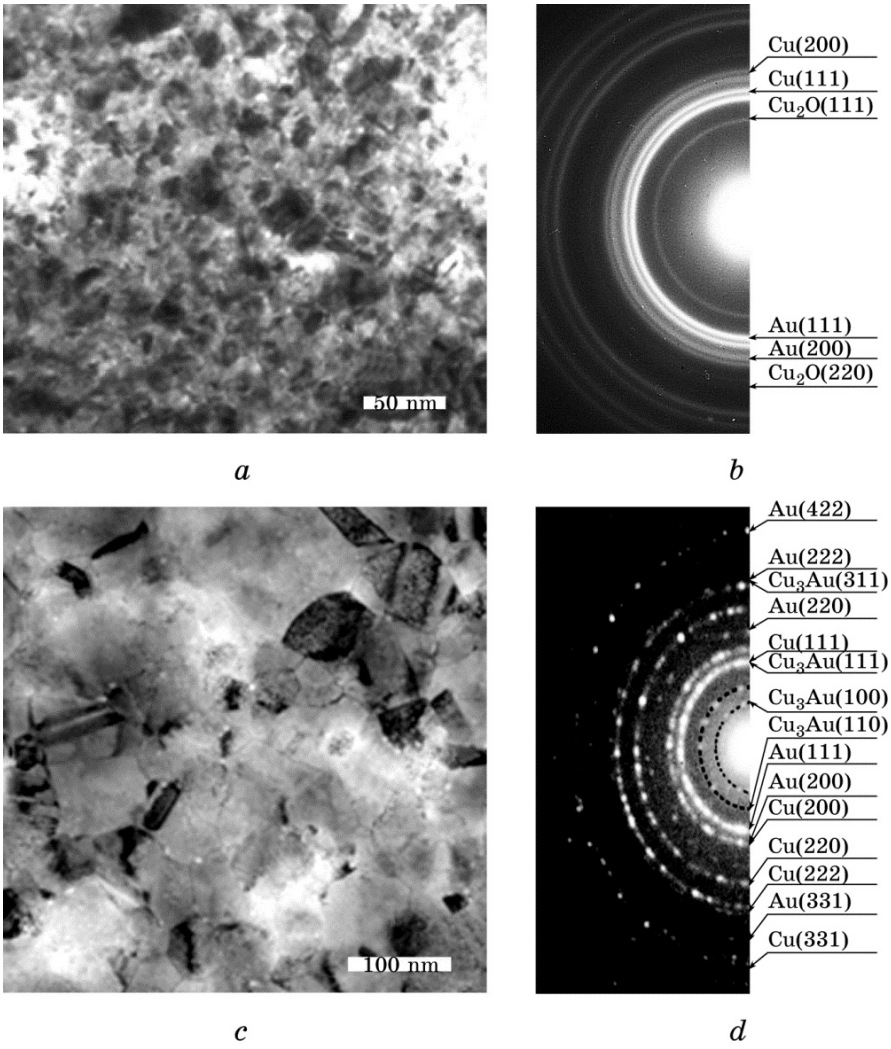

Fig. 6. Bright field images of Au/Cu bilayer as deposited (*a*) and after 15 min heat treatment at 200°C in vacuum 10^{-2} Pa (*c*). Selected area electron diffraction patterns of Au/Cu bilayer as deposited (*b*) and after 15 min heat treatment at 200°C in vacuum 10^{-2} Pa (*d*).

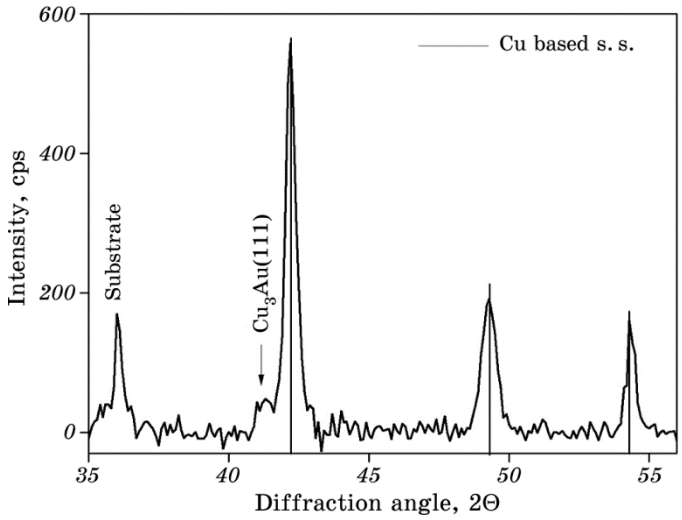

Fig. 7. XRD Θ–2Θ patterns of Au/Cu sample after annealing at 200°C for 15 min in vacuum 10^{-2} Pa.

grain sizes support this interpretation in contrast to the grain boundary motion during usual re-crystallization [30, 31].

4. CONCLUSIONS

Low-temperature interdiffusion in polycrystalline Au/Cu thin films is investigated in different atmospheres by SNMS, XRD, TEM, and AFM methods. The formation of the ordered phase Cu_3Au is observed only upon exposure in vacuum 10^{-2} Pa at 200°C, where bulk diffusion contribution is negligible. The Cu-side profiles could be interpreted supposing moving boundaries, which leave areas with high Au concentration behind themselves. According to obtained concentration profiles, the reaction layer parallel with the original interface cannot be detected. It means that compound formation takes place along grain boundaries.

ACKNOWLEDGENETS

The authors are grateful to the group of Prof. Dezső Beke for the help and assistance in SNMS investigations.

REFERENCES

1. U. Bardi, *Rep. Prog. Phys.*, **57**: 939 (1994).

2. J. H. Sinfelt, *Bimetallic Catalysts: Discoveries, Concepts and Applications* (New York: Wiley: 1983).
3. M. Ohring, *The Materials Science of Thin Films* (New York: Academic Press: 1992).
4. F. Cacho, G. Cailletaud, C. Rivero, P. Gergaud, O. Thomas, and H. Jaouen, *Mater. Sci. Eng. B*, **135**: 95 (2006).
5. K. N. Tu, *Phys. Rev. B*, **49**: 2030 (1994).
6. G. T. Galyon and L. Palmer, *IEEE Trans. Electron. Packag. Manuf.*, **28**: 17 (2005).
7. L. G. Harrison, *Trans. Faraday Soc.*, **57**: 1191 (1961).
8. W. E. Martinez, G. Gregori, and T. Mates, *Thin Solid Films*, **518**: 2585 (2010).
9. G. Schmitz, D. Baither, M. Kasparzak, T. H. Kim, and B. Krause, *Scr. Mater.*, **63**: 484 (2010).
10. V. M. Koshevich, A. N. Gladkikh, M. V. Karpovskyi, and V. N. Klimenko, *Interface Sci.*, **2**: 261 (1994).
11. U. Gösele and K. N. Tu, *J. Appl. Phys.*, **53**: 3252 (1982).
12. F. M. d'Heurle, *J. Mater. Res.*, **3**: 167 (1988).
13. T. Laurila and J. Molarius, *Crit. Rev. Solid State Mater. Sci.*, **28**: 185 (2003).
14. G. Molnár, G. Erdélyi, G. A. Langer, D. L. Beke, A. Csik, M. Kis-Varga, and A. Dudás, *Vacuum*, **98**: 70 (2013).
15. F. Hartung, J. C. Ewert, J. Dzick, and G. Schmitz, *Scr. Mater.*, **39**, No. 1: 79 (1998).
16. G. Feinstein and J. B. Bindell, *Thin Solid Films*, **62**: 37 (1979).
17. H. Oechsner, *Appl. Surf. Sci.*, **70**: 250 (1993).
18. L. Péter, G. L. Katona, Z. Berényi, K. Vad, G. A. Langer, E. Tyth-Kádar, J. Pádár, L. Pogány, and I. Bakonyi, *Electrochim. Acta*, **53**: 837 (2007).
19. A. N. Aleshin, V. K. Egorov, B. S. Bokstein, and P. V. Kurkin, *Thin Sol. Films*, **51**: 223 (1993).
20. L. A. Girifalco, *Atomic Migration in Crystals* (Tokyo, Japan: Kyōritsu Shuppan: 1980).
21. K. Maier, *phys. status solidi (b)*, **44**: 567 (1977).
22. A. Makovec, G. Erdélyi, and D. L. Beke, *Thin Sol. Films*, **520**: 2362 (2012).
23. B. D. Cullity, *Elements of X-Ray Diffraction* (Reading, MA: Addison-Wesley: 1979).
24. S. Inomata and M. O .M. Kajihara, *J. Mater. Sci.*, **46**: 2410 (2011).
25. O. Penrose, *Acta Mater.*, **52**: 3901 (2004).
26. C. Y. Ma, E. Rabkin, W. Gust, and S. E. Hsu, *Acta Metall. Mater.*, **43**: 3113 (1995).
27. F. Hartung and G. Schmitz, *Phys. Rev. B*, **64**: 245418 (2001).
28. J. Chakraborty, U. Welzer, and E. J. Mittemeijer, *J. Appl. Phys.*, **103**: 113512 (2008).
29. J. Chakraborty, U. Welzer, and E. J. Mittemeijer, *Thin Solid Films*, **518**: 2010 (2010).
30. Ya. Ye. Geguzin, Yu. S. Kaganovskiy, and L. N. Paritskaya, *Phys. Met. Metall.*, **54**: 120 (1982).
31. Yu. Kaganovskii and L. N. Paritskaya, *Encyclopaedia of Nanoscience and Nanotechnology* (Ed. H. S. Nalwa) (American Scientific Publishers: 2004), p. 1.